Engineering Structures 30 (2008) 3412–3425

Contents lists available at ScienceDirect

Engineering Structures

journal homepage: www.elsevier.com/locate/engstruct

Near surface mounted CFRP strips for the flexural strengthening of RC columns: Experimental and numerical research

Joaquim A.O. Barros [a,*], Rajendra K. Varma [a], José M. Sena-Cruz [a], Alvaro F.M. Azevedo [b]

[a] Department of Civil Engineering, University of Minho, Azurém, 4800-058 Guimarães, Portugal

[b] Department of Civil Engineering, University of Porto, Rua Dr. Roberto Frias, 4200-465 Porto, Portugal

ARTICLE INFO

Article history:
Received 21 March 2007
Received in revised form
24 January 2008
Accepted 19 May 2008
Available online 27 June 2008

Keywords:
Near surface mounted reinforcement
Reinforced concrete columns
Strengthening
Carbon fiber reinforced polymer strips
Bending failure
Epoxy adhesive

ABSTRACT

In this work, a strengthening technique based on near surface mounted (NSM) carbon fibre laminate strips bonded into slits opened on the concrete cover is used to improve the flexural capacity of columns subjected to bending and compression. This technique avoids the occurrence of the peeling phenomenon, is able to mobilize the full strengthening capacity of the strips, and provides higher protection against fire and acts of vandalism. We describe the adopted strengthening technique and report the experimental characterization of the materials involved in the strengthening process. The results obtained in two series of reinforced concrete columns, subjected to axial compression and lateral cyclic loading, show that a significant increase on the load carrying capacity can be achieved by using the NSM technique. Cyclic material constitutive laws were implemented in a finite element program and the tests with reinforced concrete columns strengthened with the NSM technique were numerically simulated under cyclic loading. These numerical simulations reproduce the experimental load–displacement diagrams satisfactorily.

1. Introduction

Until the last quarter of the twentieth century seismic loading was not generally taken into account in the design of reinforced concrete buildings or, when considered, the resulting reinforcement detailing might not be satisfactory by the standards of the current structural codes. For this reason, significant damage can occur in old buildings, even with the occurrence of moderate seismic loads. In most cases, columns represent the most vulnerable elements since their failure leads to the collapse of the structure.

Since the beginning of the nineties conventional materials used to strengthen reinforced concrete (RC) columns are being replaced with carbon and glass fibre reinforced polymers (CFRP or GFRP). The advantages of these composite materials are the strength/weight and stiffness/weight high ratios, as well as the high resistance to environmental actions, lightness, durability and ease of application [1–4].

In this work a strengthening technique, based on the installation of strips of carbon fibre reinforced polymer (CFRP) laminates into slits opened on the concrete cover of the elements to strengthen, is used to increase the flexural resistance of RC columns failing in bending. These strips have a cross section of 9.6×1.5 mm^2 and are bonded to concrete by means of an epoxy adhesive. This technique is termed near surface mounted (NSM) and its effectiveness in the flexural and shear strengthening of RC beams has been already assessed [5–10].

In recent years a significant amount of research has been undertaken with the aim of accurately modelling the cyclic behaviour of RC columns. An extensive review of available constitutive models and appropriate FEM-based numerical strategies is published elsewhere [11]. The most common approaches regarding the modelling of RC columns with finite elements involve a discretization with 3D solid elements or with Timoshenko beam elements. When 3D solid elements are used, some elements represent concrete and others simulate the reinforcement. For the case of Timoshenko beam elements each cross section is discretized into fibers, corresponding some to the concrete and the remaining to the reinforcement [12]. Models based on 3D solid elements are more suitable to reproduce the behaviour of RC columns subjected to any type of loading such as significant shear forces or torsion. Timoshenko beam based models are less demanding in terms of computational resources but are more appropriate to the simulation of columns mainly subjected to axial and flexural forces.

In the present work, the effectiveness of the NSM technique in the flexural strengthening of RC columns was appraised by means of two series of tests, with different steel reinforcement ratios, subjected to cyclic loading and constant axial compressive

* Corresponding author. Tel.: +351 253510210; fax: +351 253510217.
E-mail addresses: barros@civil.uminho.pt (J.A.O. Barros), rajendra@civil.uminho.pt (R.K. Varma), jsena@civil.uminho.pt (J.M. Sena-Cruz), alvaro@fe.up.pt (A.F.M. Azevedo).

0141-0296/$ – see front matter © 2008 Elsevier Ltd. All rights reserved.
doi:10.1016/j.engstruct.2008.05.019

Notations

The following symbols were used in the paper. Subscript s and c denote steel and concrete respectively.

C/T	Compression /Tension
$E_{c/s}$	Initial Young modulus of concrete/steel
E_{cnew}	Tangent modulus at the new stress point
$E_{so}^{+/-}$	Initial Young's modulus at reversal C/T branch
E_{cpl}	Tangent modulus when the stress is released
$E_{\text{cre}}^{-/+}$	Tangent modulus at the returning point ($\varepsilon_{\text{cre}}^{-/+}$,$f_{\text{cre}}^{-/+}$)
E_{sc}	Tangent modulus of steel
$E_{sh}^{-/+}$	Tangent modulus at strain hardening ($\varepsilon_{sh}^{-/+}$)
E_{st}	Tangent modulus of steel
$E_t^{-/+}$	Tangent modulus for concrete on C/T envelope
$f_{c/s}$	Concrete/steel stress
f_{ct}	Peak concrete tension strength
f_c'	Peak confined concrete strength
$f_c^{-/+}$	Concrete stress on the C/T envelope
$f_{\text{cnew}}^{-/+}$	New stress at the unloading strain for C/T
$f_{\text{cre}}^{-/+}$	Stress at the returning strain ($\varepsilon_{\text{cre}}^{-/+}$)
$f_{\text{csu}}^{-/+}$	Ultimate (maximum) stress during C/T in steel
$f_{\text{cun}}^{-/+}$	Unloading stress from C/T concrete envelope curve
$f_{sy}^{-/+}$	Yield stress during C/T in steel
$n_c^{-/+}$	n value for the C/T envelope curve
$R_{so}^{+/-}$	Menegotto–Pinto Eq. parameter
x_{csp}	Non-dimensional spalling strain
$x_c^{-/+}$	Non-dimensional strain on the C/T envelope
$x_{cr}^{-/+}$	Non-dimensional critical strain on C/T envelope curve.
ε_c	Concrete strain
ε_c'	Concrete strain at peak confined stress
$\varepsilon_{so}^{-/+}$	Point of origin of the C/T envelope curve
ε_{cpl}	Plastic strain
$\varepsilon_{\text{cre}}^{-/+}$	Strain at the returning point to the C/T envelope curve
$\varepsilon_{sh}^{-/+}$	Hardening strain during C/T in steel
$\varepsilon_{su}^{-/+}$	Strain at ultimate stress ($f_{su}^{-/+}$)
ε_t	Strain at peak tension stress
$\varepsilon_{\text{cun}}^{-/+}$	Unloading strain from C/T concrete envelope curve

load. These tests were numerically simulated with the materially nonlinear algorithms of the FEMIX computer code [13]. In the context of this work, additional cyclic constitutive material models were developed and implemented in the code. The RC columns are discretized with 3D Timoshenko beam elements and each cross section is treated as a set of quadrilateral sub domains (fibrous model, [12]).

In the following sections the experimental and numerical research are described and the main results are presented and discussed.

2. Experimental program

The experimental program carried out in the context of the current work is composed of eight specimens and twelve tests as shown in Table 1. Two series of columns reinforced with longitudinal steel bars of 10 and 12 mm diameter, ϕ_l, were used. The following denominations are adopted: NON series for non-strengthened columns; PRE series for concrete columns strengthened with CFRP strips; POS series for columns of the NON series which were strengthened and then retested. The generic denomination of a series is *Cnm_s*, where *n* represents the diameter of the longitudinal bars, in mm, (10 or 12), *m* is equal to *a* or *b* (*a* and *b* are two tests in similar conditions for statistical purposes), and *s* is equal to NON, PRE or POS.

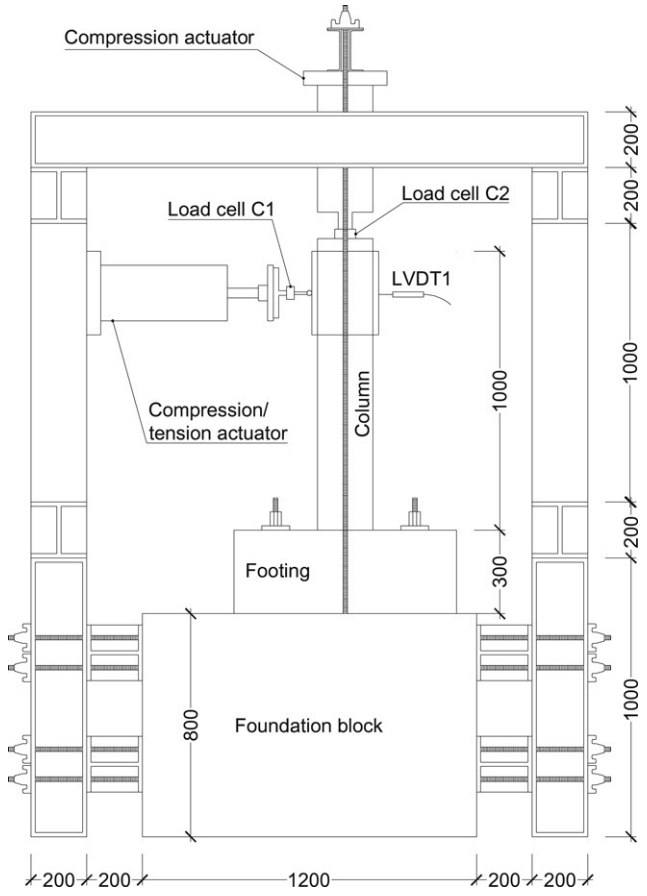

Fig. 1. Test set-up (dimensions in mm).

3. Test setup and testing procedures

The test setup is shown in Fig. 1. Each specimen is composed of a column monolithically connected to a footing, which is fixed to a foundation block by four steel bars. The cyclic horizontal load was applied by means of an actuator having a load capacity of 100 kN. The force was measured using a tension/compression load cell that can reach a maximum load of 250 kN with 0.05% accuracy. This load cell was attached to the piston of the actuator (cell C1 in Fig. 1). To avoid eccentric forces on the actuator, a 3D hinge was placed between the column and the load cell that measures the horizontal force. A vertical load of approximately 150 kN was applied to the column, which corresponds to an axial load ratio of 0.22. The vertical load was kept practically constant during the test by means of a 250 kN actuator. This actuator was supported by two bolted steel bars, which were fixed to the foundation block. The axial vertical force was measured with a 500 kN load cell with 0.5% accuracy (cell C2 in Fig. 1). Linear variable displacement transducers (LVDT) were used to record the horizontal displacements of the column, as well as an eventual vertical movement of the footing (see Fig. 2). The measuring stroke for each LVDT is indicated in parentheses ($\pm$12.5 or $\pm$25 mm). The location of the strain-gauges (SG) which were glued to the CFRP strips is also indicated in Fig. 2.

The tests were carried out with closed-loop servo-controlled equipment. A displacement history was imposed to LVDT1, with

Table 1
Denominations for the specimens

Longitudinal reinforcement (1)	Series		
	NON[a] (2)	PRE[b] (3)	POS[c] (4)
4ϕ10	C10a_NON	C10a_PRE	C10a_POS
	C10b_NON	C10b_PRE	C10b_POS
4ϕ12	C12a_NON	C12a_PRE	C12a_POS
	C12b_NON	C12b_PRE	C12b_POS

[a] Non-strengthened.
[b] Strengthened before testing.
[c] Columns of NON series after have been tested and strengthened.

Table 2
Maximum forces obtained in the columns of PRE series (strengthened before testing)

	Series PRE			
	C10a_PRE	C10b_PRE	C12a_PRE	C12b_PRE
Age[a] (days)	111	113	110	115
Average compressive strength[a] (MPa)	17.49	14.99	23.55	17.93
Tensile (kN)	37.14	40.63	44.13	39.81
Compressive (kN)	−38.54	−37.96	−43.66	−36.64

[a] Values at the age of the columns at testing.

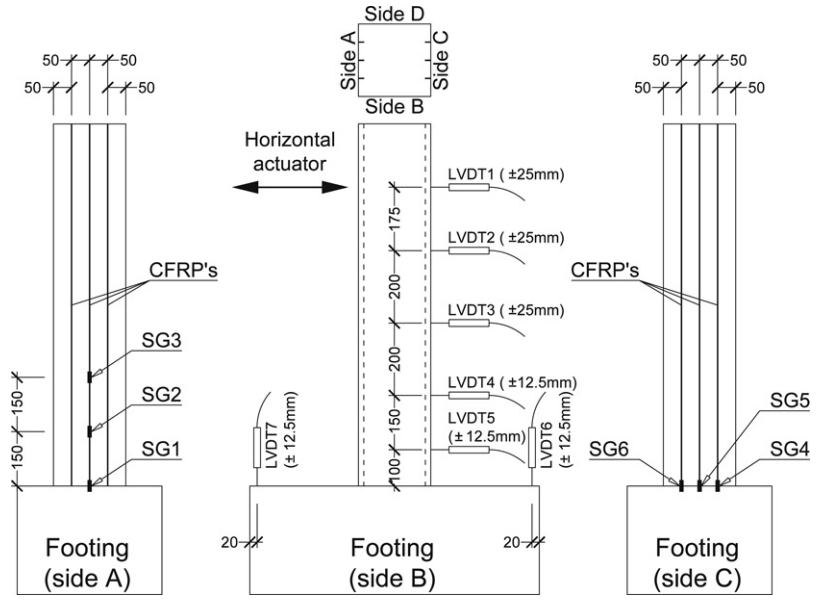

Fig. 2. Location of the displacement transducers (LVDT) and strain gauges (SG) (dimensions in mm).

a full range of 50 mm and 0.05% accuracy, located at the level of the horizontal actuator, see Fig. 1 and Fig. 2. From the analytical and numerical simulations it was verified that the steel yield initiation occurred for a lateral deflection of about 5 mm at the level of the horizontal actuator. Therefore, an increment of 2.5 mm was selected in the present experimental program. This increment was the same for all the specimens, in order to allow for the comparison of stiffness and strength degradation for the same lateral deflections. The displacement history included eight full loading-unloading cycles: ±2.5 mm, ±5.0 mm, ±7.5 mm, ±10.0 mm, ±12.5 mm, ±15.0 mm, ±17.5 mm and ±20.0 mm, with a displacement rate of 150 μm/s.

4. Material characterization

4.1. Concrete

A low strength concrete was used for all tests, in order to reproduce the type of concrete used in the sixties and seventies. The concrete was composed of 250 kg/m^3 of normal Portland cement, 1196.5 kg/m^3 of gravel 5–15 mm, 797.5 kg/m^3 of sand 0–5 mm, and 151.5 l/m^3 of water.

The uniaxial compressive behaviour of the concrete of each column series was assessed by performing compression tests with two cylinders of 150 mm diameter and 300 mm height. These tests were performed at 28 days and at the time the columns were tested. For each series of columns, two beams with dimensions of 850 × 100 × 100 mm^3 were also cast for assessing the tensile strength in bending and the fracture energy of the concrete [14]. The results obtained in the compression tests indicated an average compressive strength, at 28 days, of 16.7 MPa, with a standard deviation of 3.31 MPa. An average tensile strength of 2.62 MPa, with a standard deviation of 0.48 MPa, and an average fracture energy of 0.08 N mm/mm^2 were registered from the three-point notched beam bending tests, at 28 days. Tables 2 and 3 include the values of the concrete compressive strength at the age of the column tests.

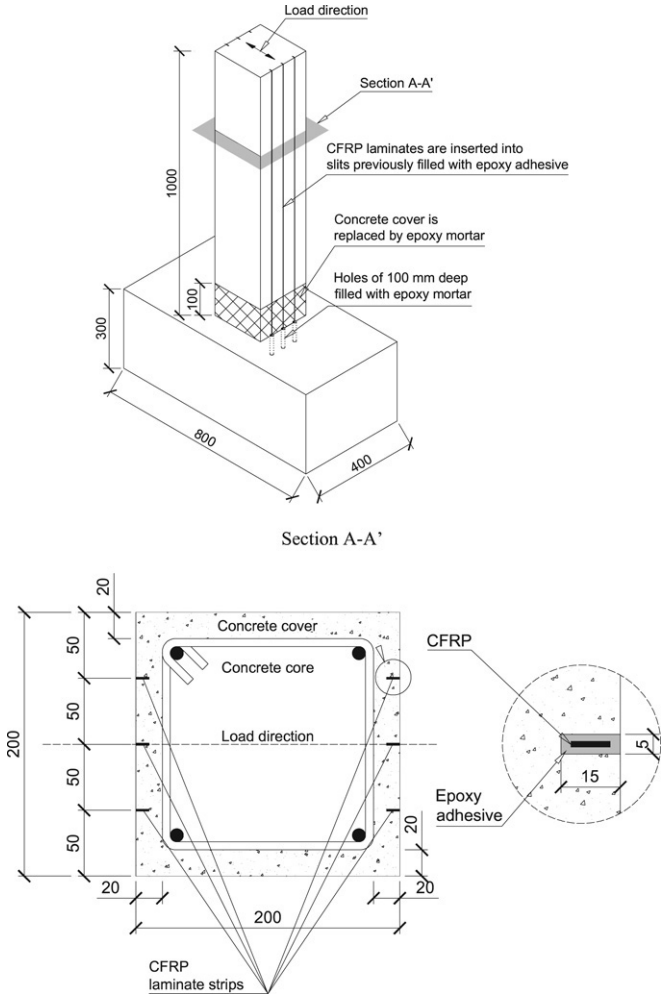

Fig. 3. Adopted flexural strengthening technique for RC columns (dimensions in mm).

4.2. Steel reinforcement

In the RC structures built in the sixties and seventies smooth surface steel bars were commonly used. For this reason, this type of bars was also used in the reinforcement of the tested columns. To assess the behaviour of the steel bars, uniaxial tensile tests were carried out in a servo-controlled testing machine, according to the recommendations of the European standard EN 10 002 [15]. The yield stress (f_{sy}), the ultimate stress (f_{su}), and the elasticity modulus (E_s) of ϕ6 bars are (as an average of the tests with three specimens): f_{sy} = 352.4 MPa, f_{su} = 352.8 MPa, and E_s = 203 700 MPa. The reinforcement details for ϕ10 and ϕ12 bars are presented later (see Table 6).

Table 3
Maximum forces obtained on the columns of series NON (non-strengthened) and POS (strengthened after preliminary testing)

Column		C10a_	C10b_	C12a_	C12b_
Diameter of longitudinal bars (mm)		10	10	12	12
Average compressive strength[a] (MPa)		15.21	13.21	17.23	19.95
Tensile	NON (kN)	16.67 (86)[b]	21.78 (85)[b]	26.35 (85)[b]	29.31 (85)[b]
	POS (kN)	37.96 (146)[b]	41.38 (130)[b]	34.11 (150)[b]	45.54 (154)[b]
	Increase (%)	127.7	89.99	29.45	55.37
Compressive	NON (kN)	−19.76 (86)[b]	−24.07 (85)[b]	−30.52 (85)[b]	−32.27 (85)[b]
	POS (kN)	−34.11 (146)[b]	−43.1 (130)[b]	−37.03 (150)[b]	−41.58 (154)[b]
	Increase (%)	72.62	79.06	21.33	28.85

[a] Values at the age of the columns at testing of the series NON.
[b] Values inside round parentheses represent the age of the columns at testing, in days.

4.3. Epoxy mortar

An epoxy mortar was used to fix the CFRP laminates to the column footing (see Fig. 3). The epoxy mortar was composed of one part of epoxy and three parts of fine sand previously washed and dried (parts measured in weight). The uniaxial compressive strength and the flexural tensile strength of the epoxy mortar were evaluated from tests in specimens with 160 × 40 × 40 mm^3, at 48 h and at 28 days, following the European standard [16]. At 48 hours, a compressive strength of 43.75 MPa, with a standard deviation of 2.14 MPa, and a flexural tensile strength of 33.93 MPa with a standard deviation of 0.57 MPa, were obtained. At 28 days, a compressive strength of 51.71 MPa, with a standard deviation of 0.47 MPa, and a flexural tensile strength of 35.40 MPa, with a standard deviation of 1.70 MPa, were obtained.

In order to evaluate the adhesive properties of the epoxy mortar relatively to a concrete surface, the following procedure was undertaken: reutilization of the remains of previous bending tests with 850 × 100 × 100 mm^3 beams, which were used to evaluate the properties of the concrete used in the columns; utilization of the epoxy mortar to glue both pieces together; test of the resulting specimen under flexure load. In these tests it could be observed that the fracture neither propagated across the epoxy mortar, nor across its interface with the concrete (see Fig. 4). Therefore, these tests indicated that the properties of the bonding between the developed epoxy mortar and concrete are very good.

4.4. CFRP laminate strips

The CFRP strips, which were provided in rolls, had a thickness of 1.45 ± 0.005 mm and a width of 9.59 ± 0.09 mm (average values of 15 measures). To evaluate the tensile strength and the elasticity

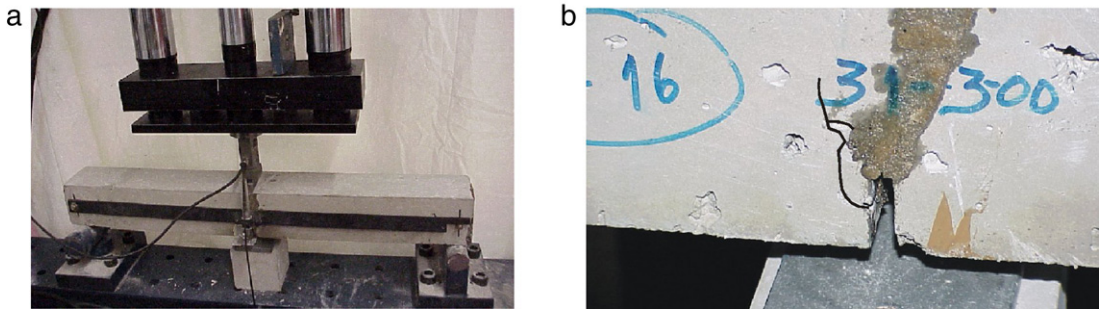

Fig. 4. Notched beam bending tests for the characterization of the concrete-epoxy mortar bond performance: (a) test setup; (b) crack propagation.

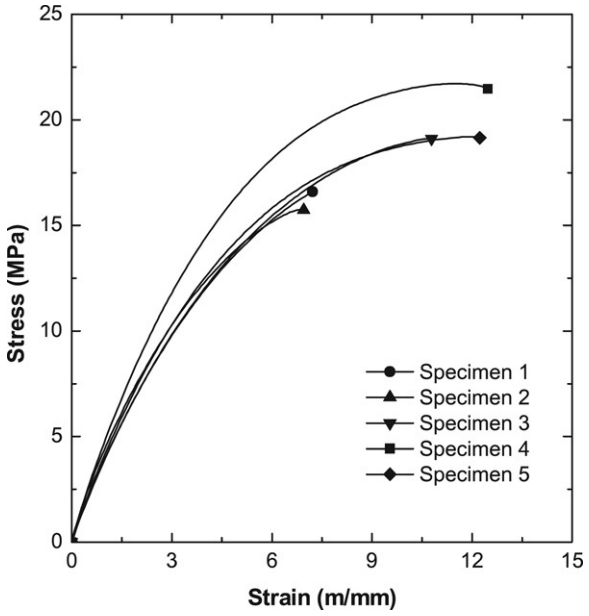

Fig. 5. Tensile stress–strain relationship for the epoxy adhesive specimens.

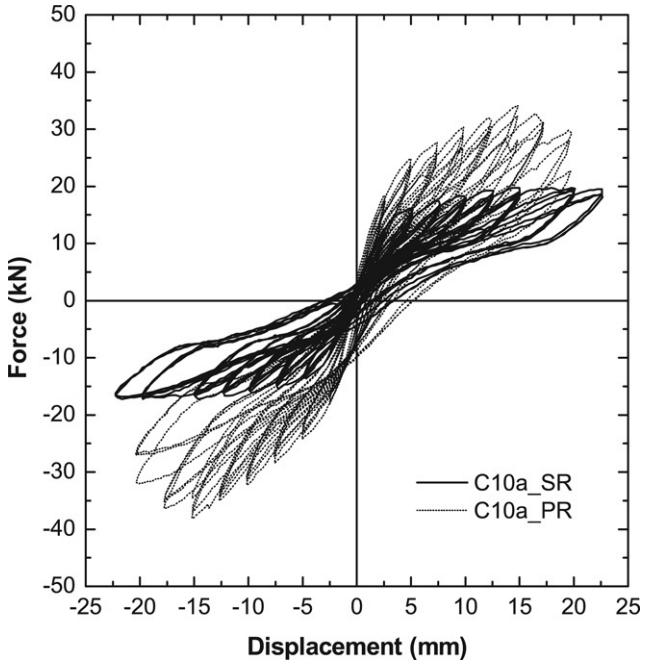

Fig. 6. Cyclic force–deflection (at LVDT1) relationship for C10a column.

modulus of the applied strips, uniaxial tensile tests were carried out in a servo-controlled test machine (Instron, series 4208), according to the recommendations of ISO 527-5 [17]. Strains were registered by means of a clip-gauge with a measuring stroke of 50 mm, whereas forces were obtained from a 100 kN load cell with an accuracy less than 0.1%. The stress–strain relationships obtained were linear up to failure, which indicates a brittle behaviour. An elasticity modulus of 159 000 MPa and a tensile strength of 1741 MPa resulted from the tests.

4.5. Epoxy adhesive

The adhesive that was used to bond the CFRP strips to concrete was composed of two parts of epoxy and one part of a hardening component (parts measured in weight). In order to assess the tensile behaviour of the epoxy adhesive, five specimens were tested with the same equipment and measurement devices that were used in the uniaxial tensile tests of the CFRP strips (see the previous Section). The tests were carried out according to the recommendations of ISO 527-2 [18] and a load cell with 5 kN load capacity was used. Fig. 5 shows the uniaxial stress–strain curves obtained in the tests. All the specimens exhibited similar uniaxial stress–strain relationships with the exception of the fourth. However, significant differences are observed in terms of tensile strength probably due to spurious voids detected in the fracture surfaces of the tested specimens. In fact, in the fracture surface of specimen 4 the imperfections were all micro-voids, while in the other specimens voids of a considerably larger size were observed. According to the recommendations of ISO 527-2 [18], an elasticity modulus of 5090 $\pm$ 590 MPa was obtained.

5. Adopted strengthening technique

Fig. 3 presents the strengthening technique adopted for the column elements. In a region 100–150 mm high at the bottom of the column (herein designated as "nonlinear hinged region") the concrete cover was removed. Afterwards, 5 mm wide and 15 mm deep slits were cut in the concrete cover, in the faces that will be subjected to the highest tensile stresses. In order to anchor the CFRP strips to the footing, 100 mm deep perforations were made in correspondence with each slit. Before the installation of the strips, all the slits and holes were cleaned using steel brushes and compressed air. The CFRP strips were cleaned with a solvent. The slits were then filled with the epoxy adhesive and the strips were installed into the slits. Finally, the nonlinear hinged region and the holes in the footing were filled with the epoxy mortar. A detailed description of this strengthening technique can be found in [19].

6. Experimental results

6.1. Load carrying capacity

The test series was carried out with the procedures described in Section 3. Tables 2 and 3 contain the extreme values obtained in the tests for the horizontal force considering as positive a right to left force in Fig. 1 (the age of the columns at testing time is in parentheses). The maximum force observed differs significantly, even between specimens of the same series. This discrepancy is mainly due to the variability of the concrete properties and to some extent lack of precision in the location of the steel reinforcement. A significant increase of the maximum load of the columns of the PRE series (strengthened before testing) and POS series (strengthened after testing) was observed, relatively to the results obtained in the columns of the NON series. As expected, the strength increase provided by the CFRP was higher in the columns with lower longitudinal steel reinforcement ratios (C10 series). The increase of the load carrying capacity provided by the NSM strengthening technique was similar in the PRE series and in previously tested columns (POS series).

6.2. Force–displacement relationships

Fig. 6 shows two typical relationships between the horizontal force and the deflection at LVDT1. The envelopes of the relationships between force and deflection at LVDT1 for all the tested columns are shown in Figs. 7 to 9. It can be observed that, in columns reinforced with ϕ10 and ϕ12 bars, the increase of the load carrying capacity occurred before and after yielding of the steel longitudinal reinforcement, respectively. Up to a deflection that approximately corresponds to the yield initiation of the steel

Fig. 7. Force–displacement envelopes for all load cycles of series C10_NON and C10_POS.

Fig. 8. Force–displacement envelopes for all load cycles of series C12_NON and C12_POS.

longitudinal reinforcement, the stiffness of the columns of the POS series was, in general, lower than the stiffness of the columns of PRE and NON series, since, when tested, the columns of the POS series were already significantly damaged. This effect is more evident in the columns possessing more longitudinal reinforcement, since, due to the higher maximum load applied to these columns, the concrete was significantly more damaged. In general, a pronounced pinching effect occurred (narrowing of the hysteretic diagrams), indicating that these columns had reduced capacity to dissipate energy. The relative high concrete compressive axial stress (3.75 MPa) and the low concrete compressive strength class applied in the tested columns have contributed to this behaviour.

Fig. 9. Force–displacement envelopes for all load cycles of series PRE.

Fig. 10. Total energy *vs.* accumulated horizontal displacement for C12b_POS column.

In the strengthened columns this pinching effect was even more pronounced since, due to the increase of the flexural carrying capacity provided by the CFRP strips, the concrete axial compressive stresses have increased. From the horizontal force *vs*. deflection at LVDT1 relationships recorded in the cyclic tests, the following diagrams can be obtained: dissipated energy *vs*. accumulated horizontal displacement, and maximum horizontal force in each series of load cycles *vs.* horizontal displacement. Typical graphs for these relationships are depicted in Figs. 10 and 11, which correspond to the C12b_POS column. Due to the fact that this strengthening technique does not provide significant concrete confinement, the increase on the dissipated energy was marginal. Table 4 includes the values of the dissipated energy obtained in the cyclic tests.